A New-Developed Nanostructured Mg/HAp Nanocomposite by High Frequency Induction Heat Sintering Process

Khalil Abdelrazek Khalil[1,2]

[1] Mechanical Engineering Department, College of Engineering, NPST, King Saud University P.O. Box 800, Riyadh 11421, Saudi Arabia
[2] Materials and Mechanical Design Department, Faculty of Energy Engineering, Aswan University, Aswan, Egypt
E-mail: kabdelmawgoud@ksu.edu.sa

The objective of the present study was to investigate the effect nano-hydroxyapatite contents on the mechanical and microstructural properties of magnesium nanocomposites in order to develop a new biodegradable hard tissue substituent. Mg/HAp nanocomposite with various HAp contents (0-10 wt %) were prepared using pure magnesium and HAp nanopowder as raw materials. The starting material was super fast densified by high frequency induction heat sintering (HFIHS). The results indicated that, a uniform distribution of HAp particles was observed along the boundary between matrix particles. Nano-crystalline grains with a crystal size range of 37-50 nm were obtained. The relative densities and microhardness of the composites initially increased with increase the amount of HAp addition. Despite the short dwelling time when the current was applied, the relative density and microhardness of the sintered samples reached as high as 99.7 % and 70 HV respectively, in the composite containing 1 to 3 wt% HAp. Addition of 1 to 3 wt% of HAp improved compression strength of Mg by 16%. Addition of HAp decreases the crystal size of the nanocomposites. The mechanical properties, i.e. hardness and compressive strength are evidently increased with increasing HAp content up to 2 wt%. However, when the HAp content was larger than 2 wt%, the compressive strength decreased due to the agglomeration of HAp particles. The hardness, compressive and ultimate stress this composite

1. INTRODUCTION

Recently, magnesium (Mg) and its alloys have attracted much attention as potential biodegradable bone implant materials due to their biodegradability in the bioenvironment [1−3]. It is characterized by non-toxicity and good biocompatibility. They are considered a novel promising

biodegradable biomaterial. Mg has the lowest density (1.74 g/cm3) of all the engineering metals with a density only slightly higher than that of plastics. Furthermore, Mg has excellent machineability; good recyclability and surface finish [4]. However, pure Mg has low elastic modulus, limited strength and creep resistance at elevated temperatures and also poor ductility due to its hexagonal crystal structure. Due to its insufficient mechanical strength, magnesium is not used in clinics up to now.

Thus, Mg is usually alloyed with other metals or used as composites [5]. It was found that Mg alloy with 3 wt% Al provides the optimal ductility and alloying with 6 wt% Al produces the optimum combination of strength and ductility [6]. Enhanced mechanical properties have been reported in Mg composite reinforced with nanoscaled ceramic particles such as SiC [7], Al_2O_3 [8] and AlN [9]. The demand for greater performance of the Mg alloys or composites leads to the development of Mg-based metal matrix composite (MMC) with nanocrystalline microstructure reinforced by in-situ ceramics [10]. Composites not only have the combined properties of their constituents, it can also be tailored to offer improved properties to meet different engineering requirements. Other elements alloying has been studied for developing biodegradable magnesium alloys with good mechanical and corrosion properties. Mn and Zn were selected as the alloying elements to develop Mg–Mn–Zn alloys due to the good biocompatibility of Mn and Zn [28, 29]. The addition of Mn and Zn improves both the mechanical properties and the corrosion resistance of magnesium alloys.

It is will known that, the composition of hydroxyapatite is similar to that of the mineral in human bone. It is excellent biocompatible, biodegradable, osteoconductive and non-toxic. But HAp is unsuitable for load-bearing implants due to its low fatigue resistance, brittleness, insufficient flexural strength and impact resistance. Hydroxyapatite is used as a coating for metal surgical implants (most often made of titanium and its alloys, or stainless steels), and recent studies have examined the possibility of its use in composite form, in materials that combine polymers with ceramic or metal/ceramic combinations. Considerable research has been performed on methods of coating application and in-situ synthesis of appetites, and the implications for ceramic properties and microstructure. Dense aggregates of HAp are typically produced by high temperature sintering or hot-isostatic pressing of sized powders (e.g., Halouani et al., [11]; van Landuyt et al. [12]; Layrolle et al.0 [13]). These studies have focused on optimizing the mechanical properties of the aggregates. However, to our knowledge, Mg/HAp nanocomposites have not been fabricated before in the literature.

On the other hand, an important reported aspect of the HFIHS process is the role of the rapid heat transfer to the product via electromagnetic waves. In previous papers [14- 21], we reported on an investigation on the consolidation and mechanical properties of different nanostructured bioceramic materials by high-frequency induction heat sintering. Unfortunately, the grain size of the sintered parts was higher than 100 nanometer. Furthermore, an exact interpretation of the microscopic effect of the HFIHS has not been achieved. In this study, a new developed Mg/HAp nanocomposite with various HAp contents (0-10 wt %) were prepared using pure magnesium and HAp nanopowder as raw materials by using HFIHS. A grain size of less than 100 nm is the main objective. The mechanical properties of the fabricated nanocomposites are accessed.

2. EXPERIMENTAL PROCEDURES

The basic configuration of a HFIHS unit is shown in Figure 1. It consists of a uniaxial pressure device, a graphite die (outside diameter, 45 mm; inside diameter, 20 mm; height, 40 mm). A water-cooled reaction chamber that can be evacuated, an induced current, pressure-, position- and temperature-regulating systems are also presented. Temperatures can be measured by a pyrometer focused on the surface of the graphite die. The system is first evacuated to a vacuum of 5×10^{-3} Torr and a uniaxial pressure is applied. An induced current (frequency of about 50 kHz) is then activated and maintained until densification observed, indicating the occurrence of the sintering and the concomitant shrinkage of the sample. Sample shrinkage could be measured by a linear gauge measuring the vertical displacement. Magnesium powder of 98.5% purity obtained from Merck KGaA, Germany, was used as the matrix material. Hydroxyapatite (HA) nanopowder of 99% purity obtained from Sigma Aldrich Corporation, USA, was used as the reinforcement. The powder has been checked for purity by X-ray diffraction as shown in Fig 2. The measured crystal size for magnesium and hydroxyapatite were 51 and 41 nm respectively. The starting grain size has been established by inspection of grain mounts using a Field Emission Scanning Electron Microscope. Fig. 3 shows FE-SEM micrographs of the used powders. Experiments have been conducted on the processing of nanostructured magnesium 1-10wt% hydroxyapatite nanocomposites and sintered by high-frequency induction heated sintering (HFIHS).
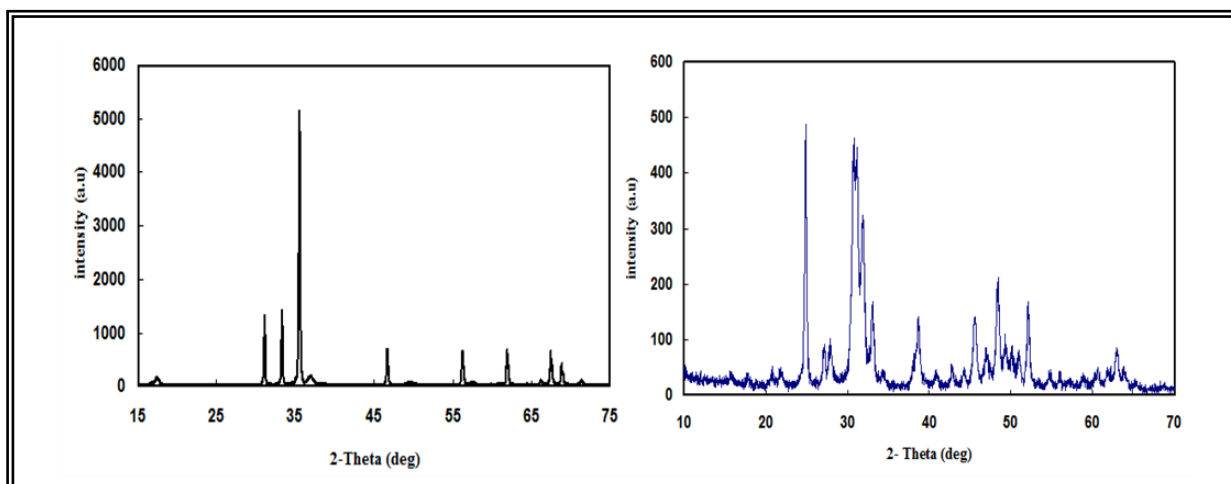
Pure magnesium and hydroxyapatite nanopowder were weighed carefully in an argon-filled glovebox. All powders were milled in FRITCSH-Germany, mechanical alloying machine using zirconia balls and a rotation speed of 200 rpm for 30 min with a ball-to-powder weight ratio of 5:1. The milling conditions were the same for all the powders. The blended powders were placed in a graphite die (outside diameter, 45 mm; inside diameter, 20 mm; height, 40 mm) and then introduced into the high-frequency induction heat sintering, shown schematically in Fig. 1. The choice of induced current was based on preliminary experiments aimed at determining the highest heating rate (highest current) that results in sample temperatures below the melting point of the material used. The samples have been densified by heating to a sintering temperature of 550 °C, and then fast cooled to room temperature within a short time. A pressure of 60 MPa was applied in two steps. In the first step the pressure was 30 MPa and maintained constant during heating, increased to 60 MPa in the second step during holding time. A heating rate of 400 °C/min was applied. After sintering, the samples were ground and polished for subsequent indentation and microscopy studies. The density of the sintered samples was measured by the Archimedes principals. Theoretical density of the Mg-HAp nanocomposites were measured based on the following equation:

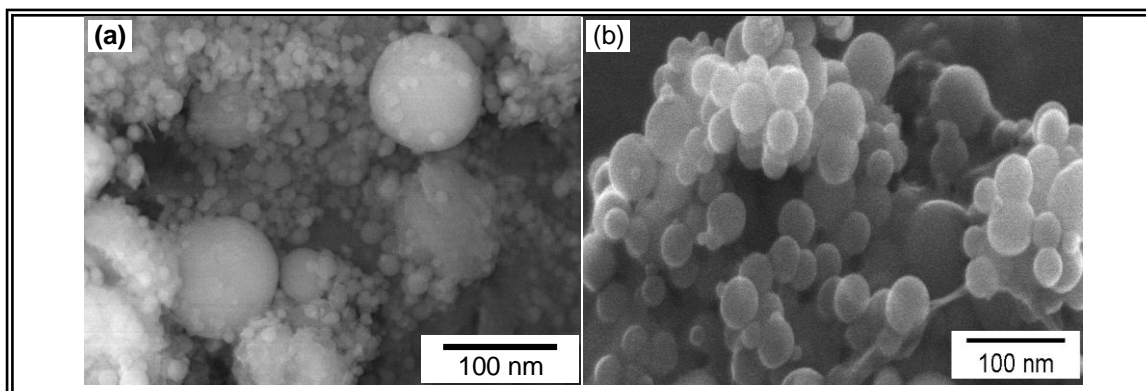$$\rho_{ave} = \frac{100}{\frac{C_1}{\rho_1} + \frac{C_2}{\rho_2}}$$

ρ_1 = ρ (HAp) = 3.16 g/cm^3, ρ_2 = ρ (Mg) = 1.74 g/cm^3.
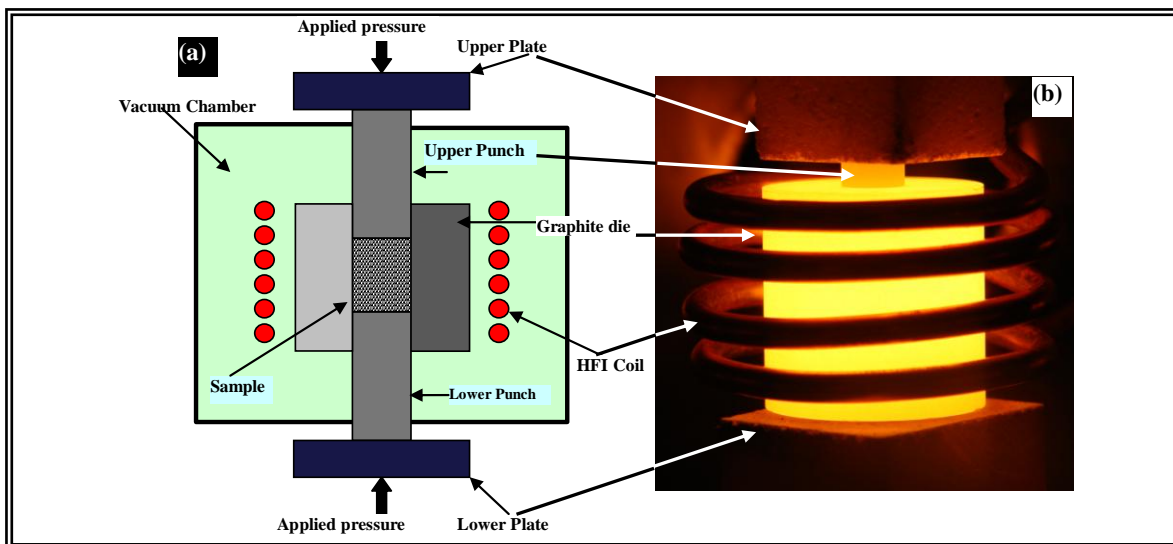
Figure 1. (a) Schematic diagram of high-frequency induction heated sintering apparatus, (b) Photo of the heated die.

Figure 2. XRD pattern of the as received magnesium and hydroxyapatite powders

Figure 3. SEM micrographs of the hydroxyapatite and magnesium powders

The microstructure observations of polished and coated fracture surfaces of the composite were investigated using a Field Emission Scanning Electron Microscope (FE-SEM) (JEOL FESEM 7600 F) coupled with EDS analysis. The surfaces were coated with platinum to avoid charging during the FE-SEM observation. Phase identification was performed on samples cut from the center of hot pressed bodies using X-ray diffractometry (XRD). X-ray diffraction analysis was carried out on the polished samples of Mg and Mg/HAp nanocomposites using an automated Shimadzu XRD-7000 diffractometer. The samples were exposed to Cu Ka radiation (k = 1.54056A˚) at a scanning speed of 2 deg/min. The Bragg angle and the values of the interplanar spacing, d, obtained were subsequently matched with the standard values for Mg, and other related phases. The crystal size of the as received powder and sintered bodies has been also determined using XRD technique. The Full Width Half Maximum (FWHM) for each peak has been detected at specific 2θ degree and evaluated using known Scherer formula. Hardness test was carried out using a Vickers diamond indenter on an automated hardness tester (Buehler, Micomet5114, Microhardness tester, Akashi, Japan). Sintered specimens of pure nano-Mg and Mg-HAp with 1.0 to 10wt.% of HAp, were tested and evaluated for their hardness. During the hardness test, a load 0.3 Kgf with a loading time of 10 s was applied to ensure that no crack propagation path was developed. Specimens used in hardness testing had average dimensions of 20 mm in diameter and 5 mm in thickness. Three samples of each of the composition type were tested for their hardness at three different locations. The average of these readings were computed, reported and compared. This determination of hardness was at ambient temperature and followed the pattern ASTM C 1421-99. To determine mechanical strength under uniaxial compressive loading, the sintered Mg-HAp specimens were tested in a fully automated tensile tester from Instron (Model 3385H, Instron Co., USA), with a constant crosshead speed of 0.5 mm/min. Compressive strength of three samples was determined and the average for each composition were calculated and compared for analysis.

3. RESULTS AND DISCUSSIONS

3.1. Characteristics of the milled powders

Figure 4 shows morphologies of the mixture of Mg−1 and 5wt% HAp powder after milling for 30 min. The as received Mg and hydroxyapatite nanopowder shown in Figure 3 before milling shows multi-crystalline and agglomerations. Compared with the initial powder, the morphology of the milled powder is similar to a spherical particle and the specific surface area is somehow decreased. Milling results in a uniform distribution of Mg and HAp powders. The refinement of grain size is resulted from the collisions between powders and balls during milling process. Specific surface area is important in relation to several factors: particle size and particle size distribution, interior pores, particle shape, agglomeration, homogeneity of the elemental powder distribution and intrinsic characteristics of powder (frangible or ductile). HAp powder is frangible whereas Mg powders are ductile. The decrease of specific surface area can result in an increase of the apparent density and tapping density.
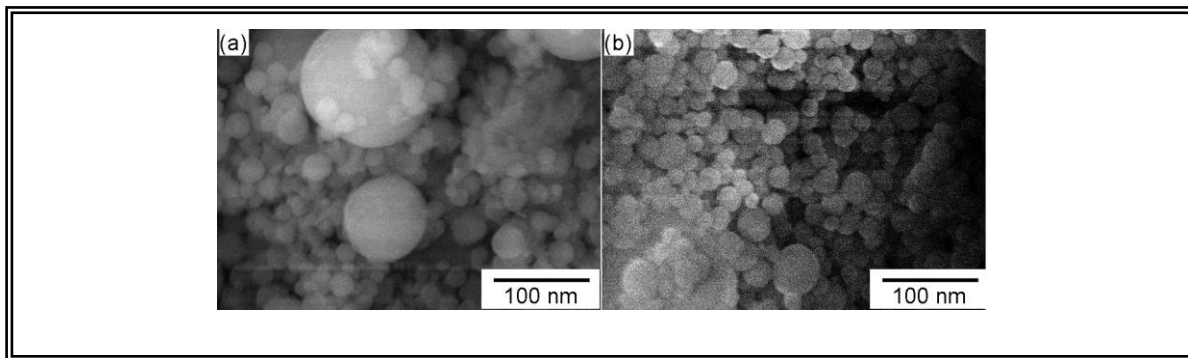
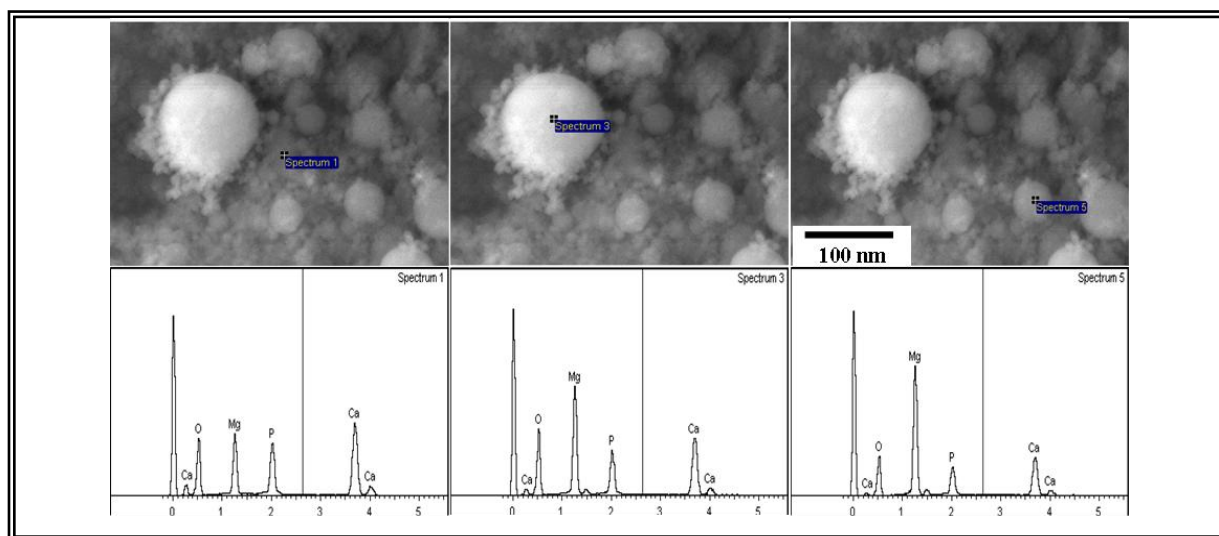**Figure 4.** FE-SEM morphology of the Mg with (a) 1wt% (b) 5wt% HAp powder mixture after milling

Figure 5. Scanning electron micrograph and EDS plots at three different locations of the Mg 5wt% HAp powder mixture after milling
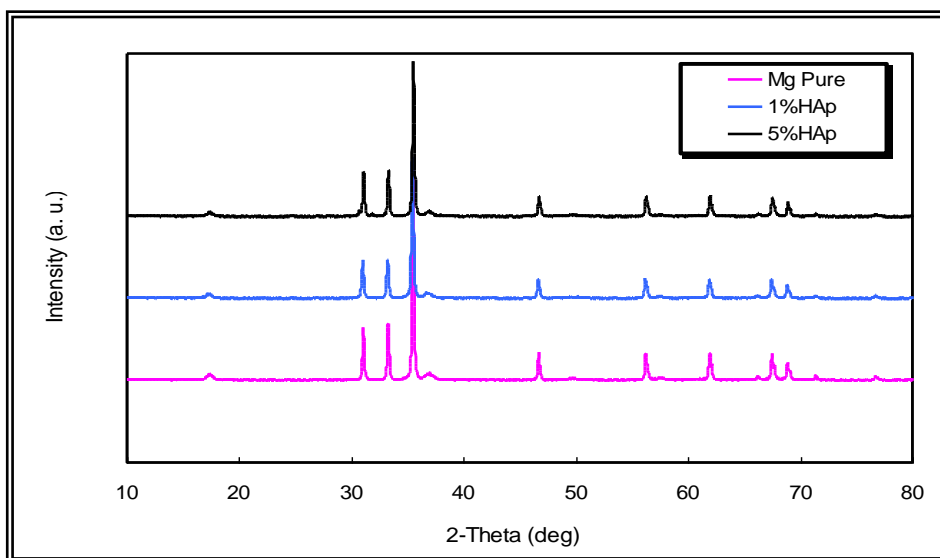

Figure 6. XRD pattern of the Mg pure and Mg with 1 and 5wt% HAp powder mixture after milling

Figure 5 shows the EDS analyses of the milled powder. It can be observed that, each Mg particle whether it is a small or large is coated with HA particles. EDS analyses clearly showed the presence of Ca, P and O of the HAp in the pure Mg structure. In addition, magnesium rich secondary phase was seen when observed at high magnification. Though the phase structure of HAp was not evident in our XRD analysis, we believe the presence of this phase was responsible for the improvement in physical and mechanical properties of Mg-HAp structures compared to pure Mg. Fig. 6 shows the XRD pattern of the milled powder. It can be seen that the width of the diffraction peaks become wider than before milling suggesting decreasing in crystal size. As was measured by Scherrer formula, the crystal size of the samples containing 1 and 5wt% HAp were 34 and 31 nm, respectively. Compared with the XRD profiles of pure Mg-HAp, the Mg phase was the main constituent phase and even there are no peaks corresponding to HAp could be observed in the milled sample due to the lower weight fraction of the reinforcement material. There is no new crystalline phase formed during the milling indicating that no chemical reactions between Mg and HAp occurred.

3.2 Effect of HAp contents on the mechanical and microstructural properties

Mg/HAp nanocomposites have been consolidated very rapidly by HFIHS at constant heating rate around 400 °C/min, constant sintering pressure (60 MPa), temperature (550 °C) and time (3 minutes holding time) in order to develop a new biodegradable hard tissue substituent possessing the advantages of the both components. The mechanical properties of the Mg/HAp nanocomposite were discussed. The results of density and relative density measurements are shown in Table 2. The results revealed that near dense pure magnesium and composite materials can be obtained using the fabrication methodology adopted in this study.

**Table 2.** Results of density and relative density measurements

Mg (C_2) (wt%)	HAp (C_1) (wt%)	Theoretical density (g/cm^3)	Measured Density (g/cm^3)	Relative Density (%)
100	0	1.740	1.727287	99.26939
99	1	1.748	1.742197	99.668
98	2	1.756	1.745886	99.42402
97	3	1.764	1.75187	99.31233
96	4	1.772	1.748808	98.69119
95	5	1.78	1.763222	99.05739

Figure 7 shows the density and microhardness of Mg-X wt% HAp sintered at sintering temperature of 550 °C, 60 MPa applied pressure and 400°C/min heating rate. The relative densities of the composites initially increased with increase the amount of HAp addition. We can see that, despite the short dwelling time when the current was applied, the relative density of the sintered samples reached as high as 99.7 % in the composite containing 1% HAp. The results of hardness measurements

revealed an increase in microhardness values with increasing weight percentage of nano-size HAp reinforcement into the magnesium matrix to a certain level and then decreased. Among the nanocomposite formulations, magnesium reinforced with 1 to 3 wt% of HAp nanopowder showed the best overall improvement in both relative density and hardness. The hardness of Mg reinforced with 1 to 3 wt% HAp 70 HV as well as the relative density reached as high as 99.7%. The reason for the increase in Relative density and microhardness is probably due to the presence of HAp fragmented nanoparticles at the grain boundary regions. These nanosized inclusions can significantly enhance the mechanical properties of Mg. Remarkably, with increasing HAp content more than 3 wt% HAp, the relative density and microhardness decreased. Decreasing in relative density and microhardness of the nano composites with increasing HAp content can be attributed to two reasons. First, some degree of HAp nanoparticle clustering takes place. Second, the sintering temperature of pure HAp is almost around 1000 °C, with increasing HAp content in the Mg matrix, 550 °C the sintering temperature become not enough for densifications. Notably, increasing sintering temperature is not possible due to low melting temperature of Mg matrix.
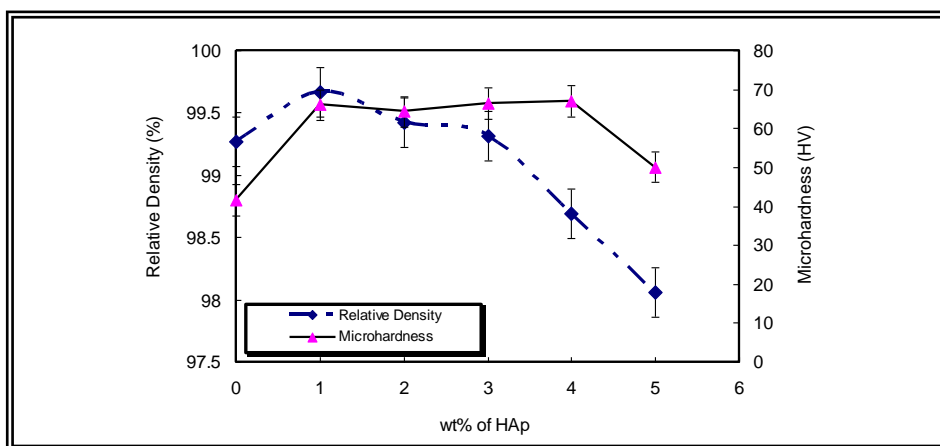
Figure 7. Effects of hydroxyapatite additions on the relative density and microhardness of Mg/HAp nanocomposites
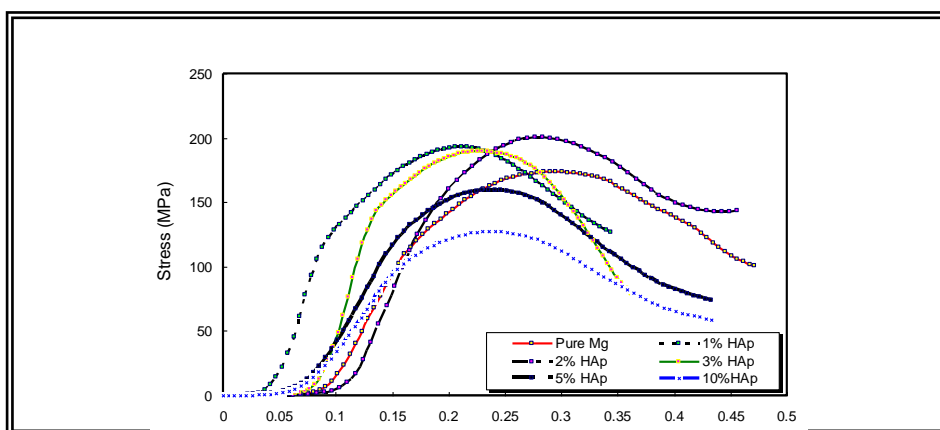

Figure 8. Typical stress–strain curve for the composites of Mg/HAp nanocomposites

The hardness values for all of the Mg/HAp nanocomposite samples have narrow distribution ranges, indicating a homogeneous distribution of the HAp phase in the Mg matrix.

Pure and nanocrystalline Mg/HAp composites, sintered at 550 °C, were subjected to mechanical testing; to determine their failure strength under uniaxial compressive loading. Sintered specimens of compositions nano-HAp, 1.0 to 5 wt% HAp were evaluated for their compression strength in a fully automated, screw driven tensile tester as shown in Fig 8. It is clear that, in the sample of Mg contains 0 wt% HAp, the value of compressive strength was low about 173 MPa in structures of pure nano-Mg, which is higher compared to compressive strength of Mg structures of sintered by conventional sintering [22-26]. However, as the amount of HAp increased, the values of compressive strength increased due to the enhancing of the nanocomposite density. Figure 9 shows the maximum compressive strength of Mg/1-10 wt% HAp. The compressive strength of the Mg/2 wt% HAp is reached as high as 204 MPa. Thus, when adding higher than 2 wt% HAp to the Mg nanocomposites, the value was again decreased to about 127 MPa with 10 wt% of HAp. Mechanical properties of Mg have been widely investigated by many researchers. Varied results have been observed and reported. More or less, these properties depend on how the structures were processed. Pressure assisted sintering as well as isostatic pressing had shown superior results. In addition, sintering temperature, time, presence of additives and their amount has played a major role in mechanical properties of sintered Mg. Recently; the arena of nanotechnology has been explored to enhanced properties of HAp as well. In a word we can conclude that, presence of HAp in the nano-Mg sintered by HFIHS further improved the mechanical strength. Addition of 1 to 3 wt% of HAp improved compression strength of Mg by 16%.
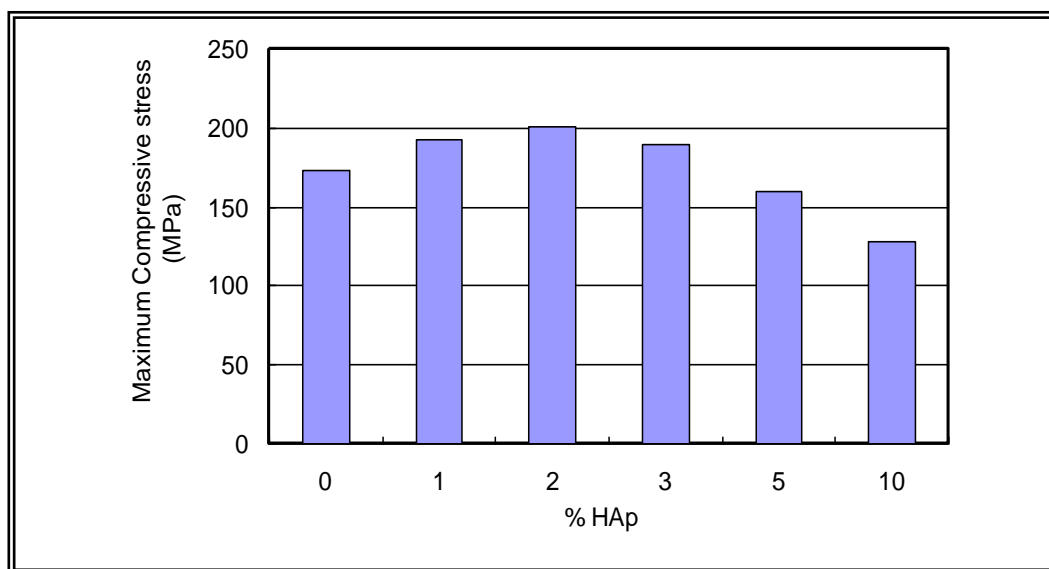
Figure 9. Maximum compressive strength of Mg with different HAp contents

X-ray diffraction analysis was carried out on the polished samples of Mg and Mg/HAp nanocomposites using an automated Shimadzu XRD-7000 diffractometer. The samples were exposed

to Cu Ka radiation (k = 1.54056A°) at a scanning speed of 2 deg/min. The Bragg angle and the values of the interplanar spacing, d, obtained were subsequently matched with the standard values for Mg, and other related phases. After filtering down the data, we can observe no any additional peaks in Mg composite reinforced with 1-5 wt% HAp that do not correspond with the pure Mg phase. Even HAp peaks were not detected in other composite formulations presumably because of its low weight fraction. The diffractograms of Pure Mg and Mg/HAp composite samples are shown in Fig. 10.

To conform prohibiting of grain growth during sintering due to using ultra fast heating rate and a very short holding sintering time, the crystal size has been calculated by using Scherrer formula as mentioned before. The average crystal size from the strongest peak has been calculated. The results of crystal size measurements are plotted against wt% HAp contents as shown in Figure 11. It is clear that, addition of HAp decreases the crystal size of the nanocomposites. This is actually because the crystal size of the starting HAp is lower than that of Mg. However, these results prove that, sintering of Mg/HAp nanocomposites by HFIHS is very effective as long as the sintering parameters could be controlled and maintained. This indicates that, the sintering efficiency of this method is very high. This high efficiency could be explained from two aspects. First, the high pressure applied could accelerate the densification process. Second, the powder is heated in a very short time with a high-temperature exposure as a result of the heat being transferred to the product via electromagnetic waves. These results prove that HFIHS is a potential method for fabricating nanocomposites at much lower temperature and within an extremely short time [19].

Microstructural characterization studies were conducted to determine grain morphology, presence of porosity, pore morphology and distribution of reinforcement. Field Emission Scanning Electron Microscope has been used. The results of microstructural characterization conducted on HFIHS sintered samples at constant sintering temperature, pressure, time and heating rate are shown in Fig. 12 through (a to f). It is clear that, Mg and Mg/1 to 3wt% HAp samples did not reveal presence of any microdefects. The outer surfaces were smooth and free of circumferential cracks. For Mg/3 to 5wt% HAp samples, the outer surfaces were comparatively rougher. The surfaces of extruded rods were smooth except for the last portion which showed the presence of shallow circumferential cracks. The results also revealed relatively uniform distribution of nano-sized HAp particulates with minimal presence of clusters (HAp particulates together but not fused with each other) in the case of samples containing low amount of HAp weight percentage (1 and 2).

Fig. 12 (a and b) and poorly distributed HAp particulates with presence of clusters and agglomerated region (HAp particulates fused with each other) in the case of samples containing high amount of HAp weight percentage (3 to 5) Fig. 12 (d to f). It was observed from the FE-SEM micrographs (Fig. 12) that particles were distributed everywhere inside the samples, either along the grain boundaries or inside the grains for samples sintered at both low and high HAp contents. In composite samples containing low content of HAp, HAp particles were well decorated along the particle/grain boundary.
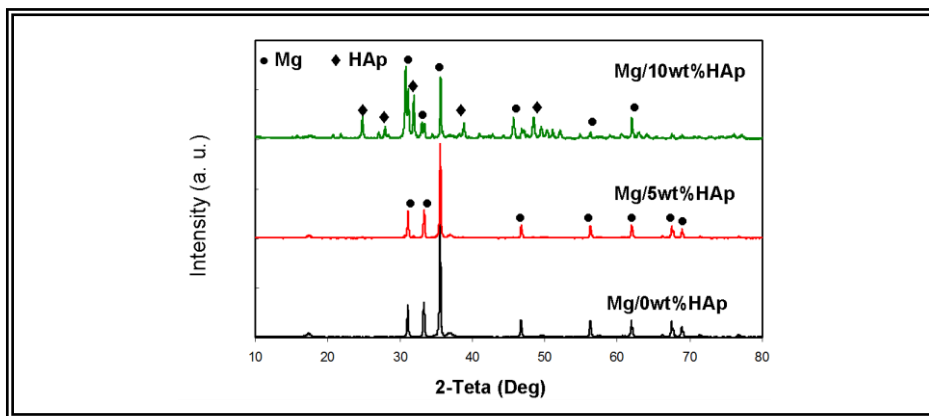
Figure 10. XRD pattern of the Mg pure and Mg with 5 and 10wt% HAp nanocomposites after sintering
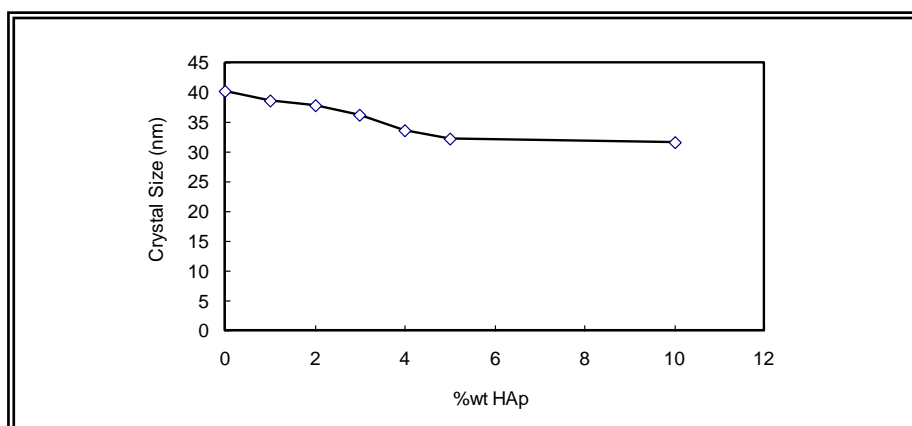
Figure 11. Crystal size measurements of the Mg/ X wt% HAp nanocomposites after sintering
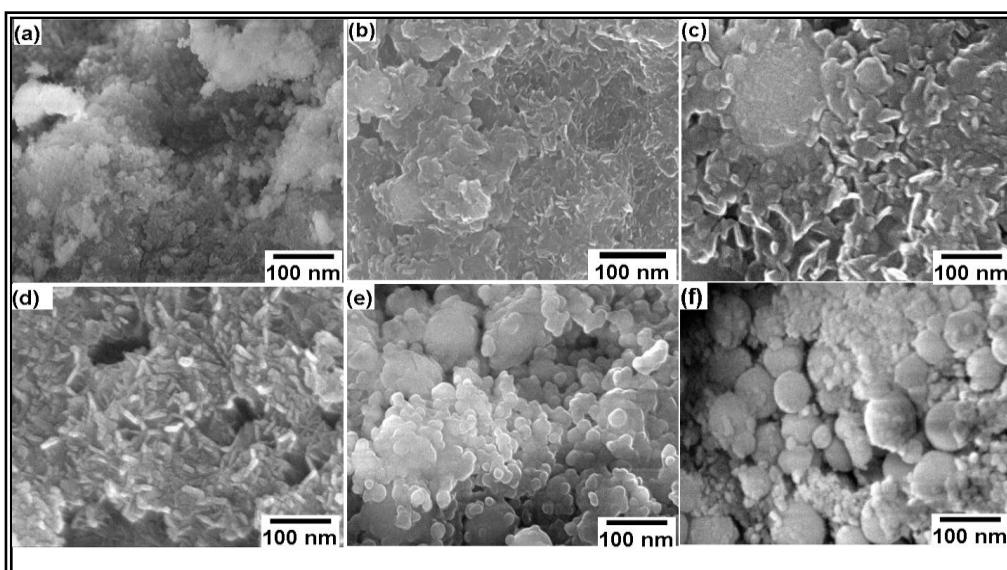
Figure 12. FE-SEM sowing the microstructure of (a) Mg-0.0%HA, (b) Mg-1.0%HA, (c) Mg-2.0%HA, (d) Mg-3.0%HA, (e) Mg-4.0%HA, and (f) Mg-5.0%HA sintered by HFIHS

4. CONCLUSIONS

Mg/HAp nanocomposites were successfully synthesized using High Frequency Induction Heat Sintering route. From the experimental results mentioned above, some conclusions were made as follows:

1.   HFIHS was effective in the preparation of fine-crystals, nearly fully dense of Mg/HAp nanocomposites from the powder with a smaller crystal size.

2.   The relative densities and microhardness of the composites initially increased with increase the amount of HAp addition. Despite the short dwelling time when the current was applied, the relative density and microhardness of the sintered samples reached as high as 99.7 % and 70 HV respectively, in the composite containing 1 to 3 wt% HAp. In the sample of Mg contains 0 wt% HAp, the value of compressive strength was low about 173 MPa in structures of pure nano-Mg. However, as the amount of HAp increased, the values of compressive strength increased due to the enhancing of the nanocomposite density. The compressive strength of the Mg/2 wt% HAp is reached as high as 204 MPa. Thus, when adding higher than 2 wt% HAp to the Mg nanocomposites, the value was again decreased to about 127 MPa with 10 wt% of HAp. Addition of 1 to 3 wt% of HAp improved compression strength of Mg by 16%.

3.   Addition of HAp decreases the crystal size of the nanocomposites. A uniform distribution of HAp particles was observed along the boundary between matrix particles. The mechanical properties, i.e. hardness and compressive strength increased with increasing HAp content up to 2 wt%. However, when the HAp content was larger than 2 wt%, the compressive strength decreased due to the agglomeration of HAp particles. The agglomeration of HAp particles was found to lead to the degradation of the interfacial bonding strength between matrix and reinforcement. However, these results prove that, sintering of Mg/HAp nanocomposites by HFIHS is very effective as long as the sintering parameters could be controlled and maintained.

References

1. W. F, Kaese V, Haferkamp H, Switzer E, Meyer-Lindenberg A, and C. J. Wirth. *Biomaterials* 26 (17): (2005); 3557–63.
2. F. Witte, J. Fischer, J. Nellesen, H. A. Crostack, V. Kaese, and A. Pisch, *Biomaterials*; 27 (7), (2006), 1013–8.
3. L. Xu, G. Yu, E. Zhang, F. Pan, and K. Yang, *J Biomed Mater Res*, 83A(3), (2007), 703–11.
4. B. Wolf, C. Fleck, D. Eifler, Int. J. Fatigue 26, (2004) 1357–1363.
5. C. Fritze, H. Berek, K.U. Kainer, S. Mielke, B. Wielage,. Fibre reinforced magnesium for automotive applications. In: Mordike, B.L., Kainer, K.U. (Eds.), Magnesium Alloys and Their Applications.Werkstoff-Information-sgesellschaft, Frankfurt, Germany, (1998) pp. 635–640.
6. M. Avedesian, H. Baker, (Eds.),. Magnesium and Magnesium Alloys. ASM International, Materials Park, OH, USA, (1999) pp. 12–25.

7. H. Ferkel, B. L. Mordike, *Mater. Sci. Eng*. A 298, (2001) 193–199.
8. S. F. Hassan, M. Gupta, *Mater. Sci. Eng*. A 392 (2005)163–168.
9. A.T. Maung, L. Lu, M. O. Lai. *Compos. Struct*. 75, (2006) 206–212.
10. S. C. Tjong, Z.Y. Ma, *Mater. Sci. Eng*. 29, (2000) 49–113.
11. R. Halouani, D. Bernache-Assolant, E. Champion, and A. Abadou. *J. Mater. Sci.: Mater. Med*., 5, (1994) 563-568.
12. V. Landuyt, P. Li, F., Keustermans, J. P., Streydio, J. M., Delannay, F., and E. Munting, *Mater. Sci.: Mater. Med.,* 6 (1995) 8-13.
13. P. Layrolle, , A. Ito, and T. Tateishi. *Journal of the American Ceramics Society*, 81, (1998) 1421-28.
14. K. A. Khalil, S. W. Kim and H. Y. Kim, *Materials Science and Engineering* A 456 (2007) 368–372.
15. S. W. Kim and K. A. Khalil, *Journal of American Ceramic Society*, Vol. 89, No. 4, (2006). p. 1280–1285
16. K. A. Khalil and S. W. Kim, Int. *Journal of Applied Ceramic Technology*, 3 [4], (2006) 322–330
17. K. A. Khalil and S. W. Kim, *Materials Science Forum Vols*. 534-536 (2007) pp. 601-604.
18. K. A. Khalil and S. W Kim, *Materials Science Forum Vols*. 534-536 (2007) pp. 1033-1036.
19. K. A. Khalil, S. W. Kim, and H. Y. Kim, *Int. Journal of Applied Ceramic Technology*, 4 [1] (2007)30–37
20. K. A. Khalil, S. W. Kim, N. Dharmaraj, K. W. Kim and H. Y. Kim, *Journal of Materials Processing Technology* 187–188 (2007) 417–420
21. K. A. Khalil, S. W. Kim, *Trans. Nonferrous Met. Soc. China*, 17(2007) 21-26.
22. W. Xie, and Y. Liu, *Journal of Alloys and Compounds* 431 (2007) 162–166.
23. W.L.E. Wong, M. Gupta, *Composites Science and Technology* 67 (2007) 1541–1552.
24. Z.R. Yang, and S.Q. Wang, *Composites:* Part A 39 (2008) 1427–1432.
25. S.F. Hassan, K. S. Tun, M. Gupta, *Journal of Alloys and Compounds* 509 (2011) 4341–4347.
26. K.S. Tun, M. Gupta, *Journal of Alloys and Compounds* 487 (2009) 76–82.